

DETERMINATION OF FCN PARAMETERS FROM DIFFERENT VLBI SOLUTIONS, CONSIDERING GEOPHYSICAL EXCITATIONS

J. VONDRÁK, C. RON

Astronomical Institute CAS - Czech Republic - vondrak@ig.cas.cz, ron@asu.cas.cz

ABSTRACT. Different VLBI solutions of celestial pole offsets (CPO) are used to determine parameters (period T and Q -factor) of Free Core Nutation (FCN). To this end, Brzeziński's broad-band Liouville equations are numerically integrated to account for geophysical excitations. Effects of the atmosphere, oceans and geomagnetic jerks (GMJ) are considered. Best-fitting values of FCN parameters are found by least-squares fit to observed CPO, corrected for the difference between the FCN parameters used in IAU 2000 model of nutation and newly estimated ones; MHB transfer function is used to compute these corrections. Out of all 42 solutions that we made the best fit is obtained for CPO from IERS C04, with only GMJ excitations considered. Estimated values of FCN parameters from this solution are $T = 430.23 \pm 0.03$, $Q = 19600 \pm 130$. Very probably, excitations of FCN by GMJ are more important than those by the atmosphere and oceans.

1. INTRODUCTION, MOTIVATION

Dominant part of nutation is caused by external torques, exerted by the Moon, Sun, and planets. Excitations by geophysical fluids (atmosphere, oceans) play much smaller role, but they are now detectable by VLBI. Rapid changes of amplitude and phase of the free term (FCN) occur near the epochs of geomagnetic jerks (rapid changes of the second time derivatives of intensity of geomagnetic field), as recently shown by Malkin (2013). We developed a method of determining FCN parameters (period T , Q -factor), considering all these effects (Vondrák & Ron, 2017). Here we apply this method to several VLBI solutions and models of geophysical excitations, and compare the results. The motivation is to demonstrate how much the solution is influenced by different VLBI solutions of CPO and different models of geophysical excitations.

2. SHORT DESCRIPTION OF THE METOD

The method is described in detail elsewhere (Vondrák & Ron, 2017), so only a very short description is given below.

We use Brzeziński's (1994) broad band Liouville equations to integrate numerically the influence of geophysical excitations, and compare the results with observed CPO. To this end, we use standard atmospheric and oceanic excitations from different sources, transformed from terrestrial to celestial reference frame (details see below). The effect of geomagnetic jerks is modeled by impulse-like excitation functions whose amplitudes are determined to yield the best agreement with observations.

Brzeziński's equations in celestial frame read, in complex form,

$$\begin{aligned} \ddot{P} & - i(\sigma'_C + \sigma'_f)\dot{P} - \sigma'_C\sigma'_f P = \\ & - \sigma_C \{ \sigma'_f(\chi'_p + \chi'_w) + \sigma'_C(a_p\chi'_p + a_w\chi'_w) + i[(1 + a_p)\dot{\chi}'_p + (1 + a_w)\dot{\chi}'_w] \}, \end{aligned} \quad (1)$$

in which $P = dX + idY$ denotes the part of CPO, caused by geophysical excitation, σ_C is the prograde Chandler frequency in terrestrial frame. σ'_C , σ'_f are the Chandler and retrograde FCN

frequencies, and χ'_p, χ'_w are the effective angular momentum functions (pressure and wind terms, respectively), all in celestial frame. All complex frequencies σ are expressed in radians per day. Numerical constants $a_p = 9.200 \times 10^{-2}$, $a_w = 2.628 \times 10^{-4}$ express different reaction on pressure and wind terms. The complex effective angular momentum functions $\chi = \chi_1 + i\chi_2$ in terrestrial frame are transformed into celestial frame, using a simple formula $\chi' = -\chi e^{i\phi}$, where ϕ is the Greenwich sidereal time; retrograde quasi-diurnal signal in terrestrial frame thus becomes long-periodic in celestial frame.

Prior to comparison, the observed CPO are corrected for the difference between the FCN parameters as used in standard IAU model of nutation and the estimated ones, to account for resonance effects. To this end, we use the Mathews-Herring-Buffet transfer function (Mathews et al., 2002):

$$T_{MHB}(\sigma) = \frac{e_R - \sigma}{e_R + 1} N_o \left[1 + (1 + \sigma) \left(Q_o + \sum_{j=1}^4 \frac{Q_j}{\sigma - s_j} \right) \right], \quad (2)$$

where σ is the frequency of nutation, e_R is the dynamical ellipticity of the rigid Earth, N, Q are complex constants, and s_j are complex resonance frequencies, corresponding to:

1. Chandler wobble CW;
2. Retrograde Free Core Nutation RFCN;
3. Prograde Free Core Nutation PFCN;
4. Inner Core Wobble ICW.

All frequencies of Eq.(2) are given in terrestrial frame and expressed in cycles per sidereal day. The most important is the resonance near RFCN, whose frequency is related to σ'_f of Eq. (1) by a simple relation $s_2 = \sigma'_f / \Omega - 1$, where $\Omega = 6.30038$ rad/day is the mean speed of Earth's rotation. When the estimated FCN parameters differ from the ones used in IAU model of nutation ($T=430.21$ d, $Q=20000$), transfer function for each nutation term changes, and so do its amplitude and phase as well as CPO. We then find the FCN parameters that yield the best fit between integrated and corrected CPO values, using standard least-squares estimation.

3. DATA USED

All data used in this study cover the same interval 1986.0–2018.5. They are as follows:

3.1 Celestial pole offsets

Celestial pole offsets (in 1-day steps), all referred to IAU2000, solutions by the following IVS analysis centers are used:

1. combined IERS C04, solution eopc04_IAU2000.dat;
2. combined IVS, solution ivs18q2X.eops;
3. Bundesamt für Kartografie und Geodäsie (BKG), solution bkg00014.eoxy;
4. Goddard Space Flight Center (GSF), solution gsf2016a.eoxy;
5. Institute for Applied Astronomy (IAA), solution iaa2017a.eops;
6. Observatoire de Paris (OPA), solution opa2019a.eops;
7. U.S. Naval Observatory (USN), solution usn2019c.eoxy.

All these data were filtered (Vondrák, 1977) to contain periods between 10 and 6000 days and centered. For FCN parameters different from the values used in IAU2000 model of nutation, these were further corrected by using MHB transfer function, as outlined above.

3.2 Atmospheric and oceanic excitations

Three different variants of excitations are used:

1. No atmospheric and oceanic excitations;

2. NCEP/NCAR atmosphere with IB correction (representing a simple oceanic model), in 6-hour steps (Zhou et al., 2006);
3. ESM GFZ atmosphere + ocean, in 3-hour steps (Dobslaw & Dill, 2018).

All excitations, originally given in terrestrial frame, were re-calculated into celestial frame, centered and smoothed to contain only periods longer than 10 days.

3.3 Excitations by geomagnetic jerks (GMJ)

Eight epochs of GMJ, found in literature are used, namely 1991.0, 1994.0, 1999.0, 2003.5, 2004.7, 2007.5, 2011.0, and 2014.0. References to corresponding papers can be found in (Vondrák & Ron, 2017). The complex amplitudes a of bell-shaped excitations, centered around these epochs and lasting 200 days, are estimated to yield the best fit to observations. The excitations have the form

$$\chi'_{\text{GMJ}} = \frac{a}{2} \left[1 + \cos \frac{2\pi(t - t_o)}{\Delta} \right], \quad (3)$$

in which t_o is equal to GMJ epochs and $\Delta = 200$ days.

4. RESULTS

We used the above described procedure, both without and with GMJ excitations, leading to 42 different solutions of period T and Q -factor. All of them are represented below graphically in Figs. 1 through 3.

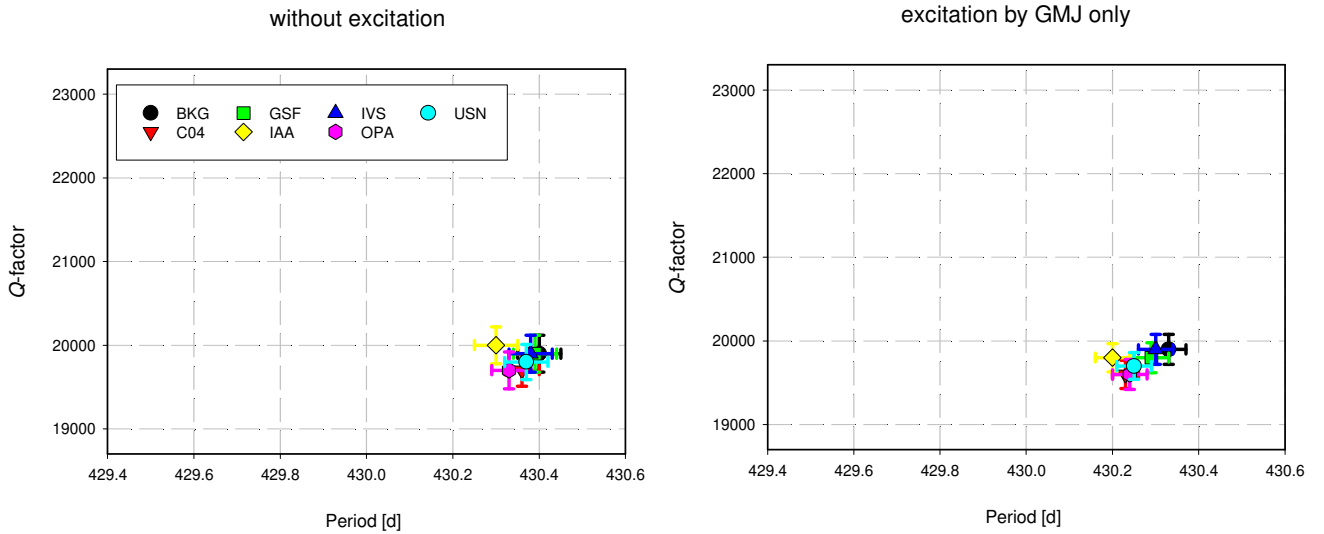


Figure 1: Solutions without atmospheric and oceanic excitations; left - no excitations at all, right - excitations by GMJ only.

Figure 1 (no atmospheric and oceanic excitations) shows clearly that all VLBI solutions yield very similar T and Q values; they agree within their formal uncertainties. The rms fit between integrated and observed CPO range from 0.232 to 0.280 mas, the best fit corresponds to IERS C04 solution. Inclusion of GMJ excitations does not change the Q -factor, and it shortens the period by less than 0.1d. It also improves the fits substantially to 0.166-0.227 mas, with the lowest value again for C04 CPO.

Figure 2 (excitations by NCEP IB atmosphere) offers a similar pattern as the preceding one; all solutions agree within their uncertainties, rms fits are slightly worse (0.246-0.351 mas for atmospheric excitation, 0.188-0.243 mas for GMJ effect added). The best fit is achieved again for

IERS C04 CPO. Difference between left and right plot is however different – Q-factor diminishes by about 1000, and period remains practically the same.

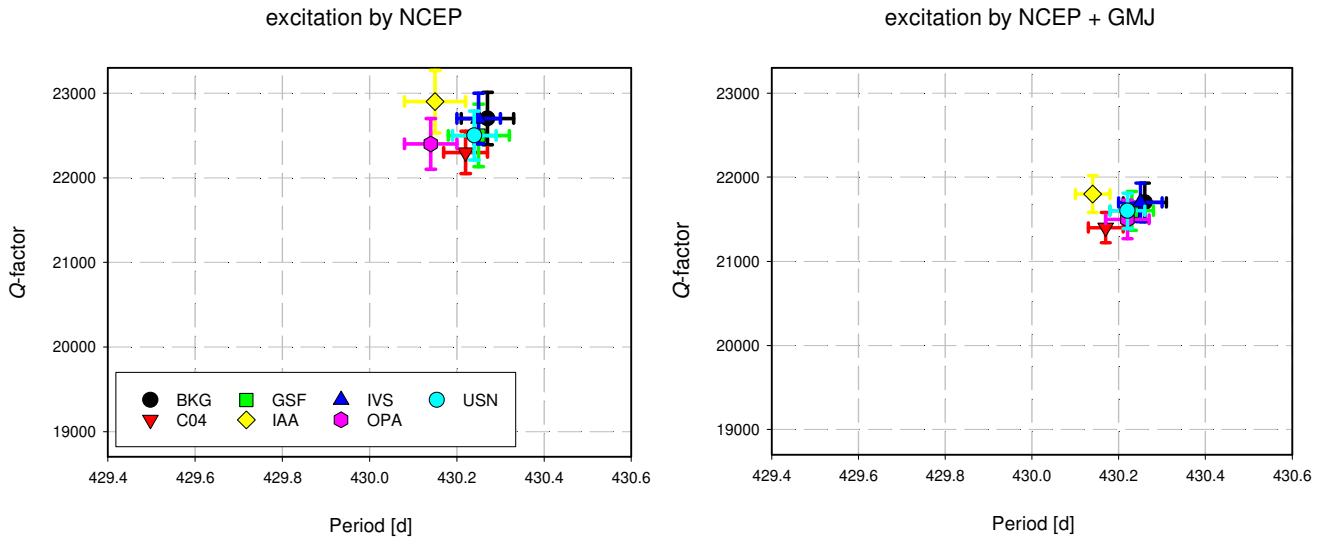


Figure 2: Solutions with atmospheric excitations NCEP IB; left - without GMJ excitations, right - with GMJ excitations.

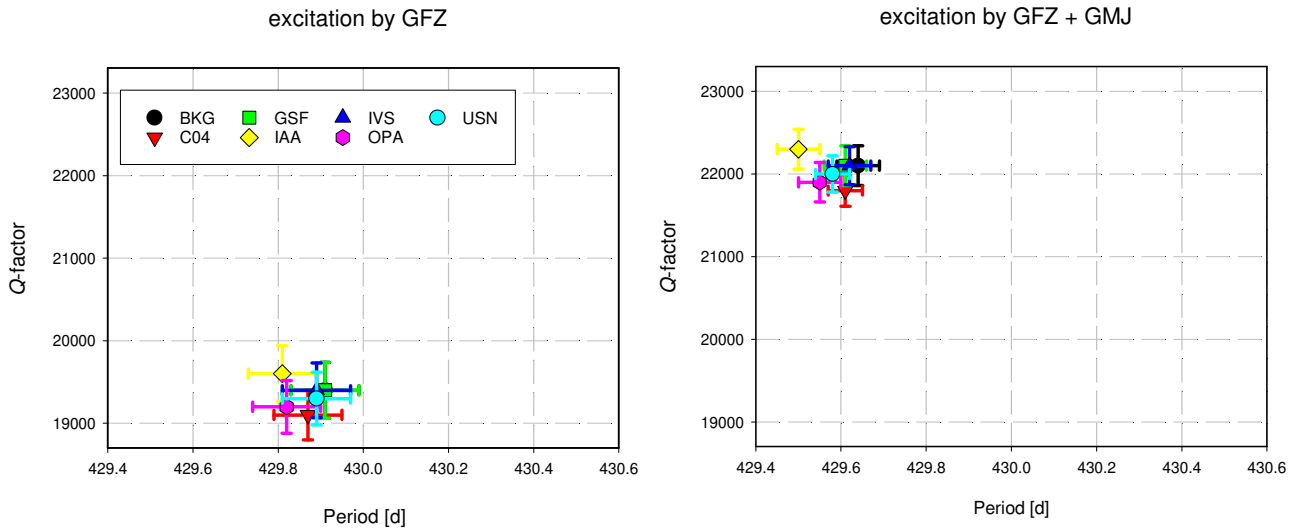


Figure 3: Solutions with atmospheric and oceanic excitations GFZ; left - without GMJ excitations, right - with GMJ excitations.

Results depicted in Figure 3 (excitations by EMS GFZ atmosphere and oceans) yield the highest values of rms fits (0.414–0.445 mas without GMJ, significantly reduced by including GMJ effect to only 0.197–0.251 mas). Similarly to Figs. 1 and 2, different CPO solutions lead to almost identical results. FCN parameters are rather different from the preceding two cases; period is shorter by about 0.3d, with GMJ excitations even more, Q-factor grows by almost 3000 if GMJ effect is added.

5. CONCLUSIONS

All results based on different VLBI solutions agree at the level of their formal uncertainties, if the same excitation model is used. The best rms fit to observations is always obtained with IERS C04 solution. Different models of excitation yield values of FCN parameters whose differences often exceed their formal errors. Quite surprisingly, the best fit is obtained when atmospheric and oceanic excitations are neglected. Inclusion of GMJ effect always improves the fit, the most significant improvement occurs in case of EMS GFZ excitations, but in some cases it brings about relatively large changes of FCN parameters, exceeding their formal errors. Out of our 42 solutions the best fitting one is based on CPO from IERS C04, when only GMJ excitations are considered: $T = 430.23 \pm 0.03$, $Q = 19600 \pm 130$, with rms fit to observations 0.166 mas. Thus it seems that the excitations by GMJ are probably more important than the ones by atmosphere and oceans.

6. REFERENCES

- Breziński, A., 1994, "Polar motion excitation by variations of the effective angular momentum function: II. Extended Model", *Manuscripta geodaetica* 19, pp. 157–171.
- Dobslaw, H., Dill, R., 2018, "Predicting Earth orientation changes from global forecasts of atmosphere-hydrosphere dynamics", *Adv. Space Res.* 61, 4, pp. 1047–1054, doi: 10.1016/j.asr.2017.11.044.
- Malkin, Z., 2013, "Free core nutation and geomagnetic jerks", *J. Geodyn.* 72, pp. 53–58, doi: 10.1016/j.jog.2013.06.001.
- Mathews, P.M., Herring, T.A., Buffet, B.A., 2002, "Modeling of nutation-precession for nonrigid Earth, and insights into the Earth's interior", *J. Geophys. Res.* 107, B4, doi: 10.1029/2001JB000390
- Vondrák, J., 1977, "Problem of smoothing observational data II", *Bull. Astron. Inst. Czechosl.* 28, pp. 84–89.
- Vondrák, J., Ron, C., 2017, "New method for determining free core nutation parameters, considering geophysical effects", *A&A* 604, A56, doi: 10.1051/004-6361/201730635.
- Zhou, Y.H., Salstein, D.A., Chen, J.L., 2006, "Revised atmospheric excitation function series related to Earth variable rotation under consideration of surface topography", *J. Geophys. Res.* 111, D12108, doi:10.1029/2005JD006608.